analytical chemistry

pubs.acs.org/ac

Article

Development of a Low-Cost Cotton-Tipped Electrochemical Immunosensor for the Detection of SARS-CoV-2

Shimaa Eissa and Mohammed Zourob*

Cite This: https://dx.doi.org/10.1021/acs.analchem.0c04719

Read Online

ACCESS | Metrics & More | Article Recommendations

ABSTRACT: Collection of nasopharyngeal samples using swabs followed by the transfer of the virus into a solution and an RNA extraction step to perform reverse transcription polymerase chain reaction (PCR) is the primary method currently used for the diagnosis of COVID-19. However, the need for several reagents and steps and the high cost of PCR hinder its worldwide implementation to contain the outbreak. Here, we report a cotton-tipped electrochemical immunosensor for the detection of severe acute respiratory syndrome coronavirus 2 (SARS-CoV-2) virus antigen. Unlike the reported approaches, we integrated the sample collection and detection tools into a single platform by coating screen-printed electrodes with absorbing cotton padding. The immunosensor was fabricated by immobilizing the virus nucleocapsid (N) protein on carbon nanofiber-modified screen-printed electrodes which were functionalized by diazonium electrografting. The detection of the virus antigen was achieved via swabbing followed by competitive assay using a fixed amount of N protein antibody in the solution. A square wave voltammetric technique was used for the detection. The limit of detection for our electrochemical biosensor was 0.8 pg/mL for SARS-CoV-2, indicating very good sensitivity for the sensor. The biosensor did not show significant cross-reactivity with other virus antigens such as influenza A and HCoV, indicating high selectivity of the method. Moreover, the biosensor was successfully applied for the detection of the virus antigen in spiked nasal samples showing excellent recovery percentages. Thus, our electrochemical immunosensor is a promising diagnostic tool for the direct rapid detection of the COVID-19 virus that requires no sample transfer or pretreatment.

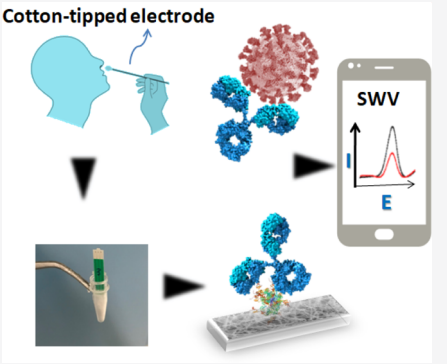

INTRODUCTION

The newly identified severe acute respiratory syndrome coronavirus 2 (SARS-CoV-2) is the last discovered member of corona viruses that cause serious human respiratory infections. Other types of corona viruses were previously known, such as the Middle East respiratory syndrome coronavirus, SARS-CoV1, HCoV-OC43, HCoV-229E, HCoV HKU1, and HCoV NL63.[1] Since its first identification in China in 2019 until present, SARS-CoV-2 has spread globally causing significant morbidity and mortality. COVID-19, the disease caused by SARS-CoV-2, was declared as a pandemic by the World Health Organization on March 2020. Until now, there are no available vaccines or drugs proven to treat COVID-19. Therefore, the timely detection of SARS-CoV-2 is urgently needed to effectively control the rapid spread of the infection.

Several diagnostic methods are being developed for the detection of COVID-19. It can be achieved by the reverse transcription polymerase chain reaction (RT-PCR) test, detection of antigens, or by serological testing (the detection of the virus antibody). However, the serological tests are not reliable for the early diagnosis of SARS-CoV-2 infection because of the relatively long delay between infection and seroconversion. Molecular diagnosis using RT-PCR is the primary used method for the detection of corona viruses. However, PCR takes relatively long time for analysis (minimum of 3 h) and requires several steps, including the collection of the specimens by swabbing, the transport of the sample into a solution, and extraction of the viral RNA before amplification. Moreover, RT-PCR is relatively expensive which hindered its wide applicability for population scale diagnosis of SARS-CoV-2, particularly in low- and middle-income countries.[1] Thus, sensitive, rapid, and accurate diagnostic methods based on the direct detection of the viral antigen without pretreatment are highly demanded to control the COVID-19 outbreak. There are four main structural antigens for corona viruses: nucleocapsid (N), spike (S), matrix (M), and envelope (E). Among them, the S and N proteins have the potential to be used as biomarkers because they can distinguish different types of corona viruses.[2]

Received: November 9, 2020
Accepted: December 15, 2020

Scheme 1. Schematic of the Cotton-Tipped Electrochemical Immunosensor for COVID-19; (A) Sample Collection Using the Cotton-Tipped Electrode, (B) Functionalization of the Carbon Nanofiber Electrode Using Electroreduction of Diazonium Salt and the Attachment of the Virus Antigen, (C) Detection Principle Using Competitive Assay and SWV Technique

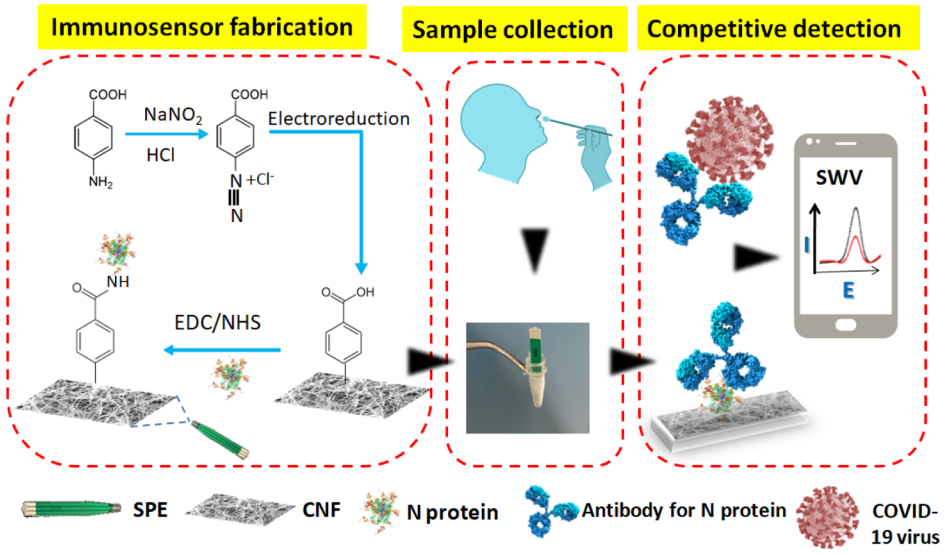

Biosensors have been widely used for many diagnostic applications showing fast, easy, and reliable detection.[3−5] Several types of biosensors have been previously reported for the detection of viruses using surface plasmon resonance,[6−9] electrochemical,[10−12] and colorimetric lateral flow assay (LFA)[13,14] detection. Until now, only few biosensors have been developed for the detection of SARS-CoV-2 such as the graphene-based field-effect transistor (FET) biosensor reported by Seo et al.[15] The FET immunosensor was used for the detection of SARS-CoV-2 using spike S1 protein as the biomarker. Plasmonic photothermal biosensors for SARS-CoV-2 through nucleic acid hybridization have been also developed.[16] Fluorescence-based microfluidic immunoassays for the detection of SARS-CoV-2 antigens and antibodies have been also reported.[17] Despite the sensitivity of these sensors, they still need either an extraction step of the RNA and/or expensive equipment for measuring the signals.

A half-strip LFA for the detection of N protein was recently reported.[18] Another lateral flow strip membrane assay was also reported for the simultaneous detection of RdRp, ORF3a, and N genes from the PCR product.[19] However, LFA provides qualitative or semiquantitative results and more work is still required to develop more accurate detection methods.

Electrochemical biosensors are one of the most popular types of biosensors which offer several advantages such as the low cost, capability of miniaturization, and high sensitivity and selectivity. These advantages make them ideal for use as point-of-care devices for diagnostic applications. Nucleic acid-based electrochemical biosensors have been lately developed for the detection of the SARS-CoV-2 N protein gene using gold nanoparticle-modified electrodes.[20] This method showed good sensitivity; however, it still requires an RNA extraction step prior to the detection that needs special reagents and trained personnel.

Electrochemical biosensors have been widely integrated with carbon nanostructures to fabricate highly sensitive devices. A carbon nanofiber (CNF) is one of the materials that showed excellent applications in biosensors because of its large surface area, stability, and ease of functionalization.[21,22]

Cotton swabs have been recently used in the fabrication of immunoassays for the detection of different pathogens.[23−25] In these assays, the colorimetric detection was achieved based on visual discrimination of the color change. These assays are simple, fast, and easy to perform. However, they only give qualitative or semiquantitative results. Thus, more accurate methods are still required.

Here, we report for the first time the combination of cotton fibers and electrochemical assays for the detection of SARS-CoV-2 antigen. The cotton-tipped electrochemical immunosensor plays dual function roles as sample collector and detector allowing the rapid, simple, and low cost detection of the virus without prior sample preparation. CNF-modified screen-printed carbon electrodes were used for the immunosensor fabrication on which N antigen was immobilized after functionalization of the sensor surface by electrografting. Competitive assay was used for the detection of the N protein showing excellent sensitivity and selectivity. The electrochemical detection can be performed using a handheld potentiostat connected to a smartphone for the signal reading.

EXPERIMENTAL SECTION

Materials and Reagents. Potassium ferricyanide [$K_3Fe(CN)_6$], potassium ferrocyanide [$K_4Fe(CN)_6$], 4-aminobenzoic acid, hydrochloric acid, sodium nitrite, bovine serum albumin (BSA), and phosphate buffer saline (PBS) were obtained from Sigma (Ontario, Canada). *N*-Hydroxysuccinimide (NHS), 1-ethyl-3-(3-dimethylaminopropyl) carbodiimide hydrochloride (EDC), and PCR tubes were purchased from Fisher Scientific (Ontario, Canada). CNF powder was obtained from Metrohm DropSens, Inc. (Asturias, Spain). The antigen of SARS-CoV-2 [nucleocapsid protein (N protein)] and its antibody were purchased from Sino Biological (Beijing, China). Influenza A antigen (N1H1) (no. J8034) was purchased from BiosPacific (CA, USA). HCoV antigen (HK41 N) and its antibody were obtained from Medix Biochemica (Finland). Sterile cotton was obtained from local pharmacy in Riyadh city. 1× PBS buffer (pH 5.5) was used for the preparation of EDC/NHS solution for the activation step.

https://dx.doi.org/10.1021/acs.analchem.0c04719
Anal. Chem. XXXX, XXX, XXX−XXX

1× PBS buffer (pH 7.4) was used for the preparation of the antigens and antibody solutions and washing steps. The CNF solution was prepared by dispersion of 1 mg of the CNF powder in 1 mL of DMF with sonication for 30 min until a homogeneous solution is obtained. All the solutions were prepared using Milli-Q water.

Instrumentation. An Autolab potentiostat, PGSTAT302N from Metrohm (Switzerland), was used to perform all the electrochemical measurements [the cyclic voltammetry (CV) and square wave voltammetry (SWV)]. Disposable screen-printed electrodes (PCR P01) adopted for PCR tubes were purchased from BioDevice Technology (Nomi, Japan). Each electrode consists of rectangle-shaped carbon working and counter electrodes and a central silver/silver chloride (Ag/AgCl) reference electrode. The electrical contacts are made of silver. The ends of the electrodes were designed to fit into the standard PCR tubes. The electrodes were connected to the potentiostat through a connector obtained from BioDevice Technology. The morphology of the CNF-modified electrodes was examined via scanning electron microscopy (SEM) measurements using an acceleration voltage of 5 kV, magnification = 12,000×, and a working distance of 9.8 mm.

METHODS

Modification of the Carbon Electrodes with CNFs. A drop casting method was used to modify the carbon working electrode of the screen-printed chip. 0.5 μL of the CNF solution in DMF (1 mg/mL) was placed on the surface of the working electrodes. The electrodes were then left to dry at room temperature for at least 20 h. Then, the electrodes were gently washed with water to remove the excess CNF and dried.

Functionalization of the CNF-Modified Electrodes Using Electrografting. The CNF surface was then functionalized using electrografting of carboxyphenyl groups via the reduction of diazonium salt, as previously reported on different carbon materials.[26,27] Briefly, as shown in Scheme 1, 2 mM of 4-aminobenzoic acid solution were mixed with 2 mM of sodium nitrite solution in 0.5 M HCl with stirring for 10 min at room temperature to produce the diazonium salt. A total of 100 μL of the diazonium solution was then added into a PCR tube in which the CNF electrode was immersed from one end and the other was connected to the potentiostat to perform electroreduction using two CV scans from +0.2 to −0.7 V at a scan rate of 50 mV s^{-1}. The chips were then washed with water and dried. To confirm the success of the grafting step of the carboxyphenyl groups on the electrode surface, X-ray photoelectron spectroscopy (XPS) measurements were recorded for the CNF-modified electrodes before and after the electroreduction step.

Immobilization of the Nucleocapsid Antigen on the Functionalized Electrodes and Preparation of the Cotton-Based Electrochemical Sensor. The carboxyphenyl-modified CNF electrodes were incubated in PBS buffer (pH 5.5) containing 100 mM EDC and 20 mM NHS for 1 h at room temperature in order to activate the terminal carboxylic groups. After that, the electrodes were washed with PBS buffer (pH 7.4) and incubated individually at room temperature with 10 μg/mL of the SARS CoV-2 antigen solution in PBS buffer (pH 7.4) for 3 h in a water-saturated atmosphere. Finally, the antigen-coated electrodes were then rinsed using PBS buffer and incubated in a solution of 0.1% BSA in PBS buffer (pH 7.4) for 30 min to block the free sites on the electrode surface.

After immobilizing the antigens, the cotton-tipped immunosensors were prepared by covering the tapering end of the electrode containing the detection zone with a piece of cotton fiber (30 mg) without scratching the sensor surface. The prepared immunosensors can be used immediately for collecting the nasal sample (Scheme 1) or kept dry at 4 °C until further use.

Electrochemical Competitive Detection of SARS-CoV-2 Nucleocapsid Antigen on the Cotton-Based Immunosensor. For the detection of the standard antigen solutions in PBS buffer, different concentrations (0.1 pg/mL to 1 μg/mL) of the N protein were first mixed with 10 μg/mL solution of the N protein antibody in PBS buffer (pH 7.4) off the chip in an Eppendorf tube. Then, 100 μL of the mixture was added to a PCR tube in which the cotton-tipped immunosensor was then immersed and incubated for 20 min at room temperature. After the incubation, the immunosensor was taken out and placed in another PCR tube containing 100 μL of PBS buffer and left for 1 min for washing. Then, the cotton electrode was placed on the absorbing cotton pad to remove the excess washing solution. Finally, the immunosensor was immersed into a PCR tube containing 10 mM of the redox solution (ferro/ferricyanide) in PBS buffer (pH 7.4) to maintain all electrodes in contact with the solution during the SWV measurements. The electrochemical sensor response was calculated as $(i - i^{o})/i^{o}$ %, where i is the reduction peak current of the electrodes after incubation with the mixture of the antigen and antibody solution and i^{o} is the original peak current of the immunosensor before incubation.

Electrochemical Measurements. The SWV measurements were recorded in 10 mM 1:1 ferro/ferricyanide solution in 10 mM PBS buffer (pH 7.4). The scanning potential range of the SWV is from 0.3 to −0.5 V at step potential of −5 mV, amplitude of 20 mV, and frequency of 25 Hz. Base-line corrections were performed for all the SWV curves. The CV for the diazonium electroreduction was performed at a scan rate of 50 mV s^{-1} by CV scanning from +0.2 to −0.7 V.

Cross-Reactivity Testing of the Immunosensors with Other Antigens. In order to study the selectivity of the SARS-CoV-2 immunosensor toward its antigen, the immunosensor was tested against Flu A and HCoV antigens. The test was performed by mixing 10 μL of SARS-CoV-2 antibody (10 μg/mL) with 10 μL of Flu A or HCoV antigens (1 ng/mL). Then, the mixtures were incubated with the SARS-CoV-2 immunosensor for 20 min and then washed. The sensor response in each case was evaluated as described above.

Testing of the Immunosensors on Spiked Nasal Fluid. The cotton-tipped immunosensor was used to collect nasal fluid from healthy volunteer (one of the authors). Then, the immunosensor was immersed in a PCR tube containing 50 μL of 10 μg/mL solution of the antibody spiked with 50 μL of 0.001 or 100 ng/mL of the protein solution in PBS buffer (pH 7.4). The immunosensors were incubated for 20 min, then washed and measured by SWV, as described above.

Preparation of Clinical Samples. Three clinical samples were used in this study. Nasopharyngeal swabs from patients and healthy/normal individuals were collected and stored in universal transport media (UTM) (IRB registration number: 20-#1276E). The samples were initially tested using real-time (RT-PCR) to determine the positive and negative ones. The samples were inactivated and kept at −80 °C until further use. For the detection, the samples were diluted 1:10 in PBS buffer

https://dx.doi.org/10.1021/acs.analchem.0c04719
Anal. Chem. XXXX, XXX, XXX−XXX

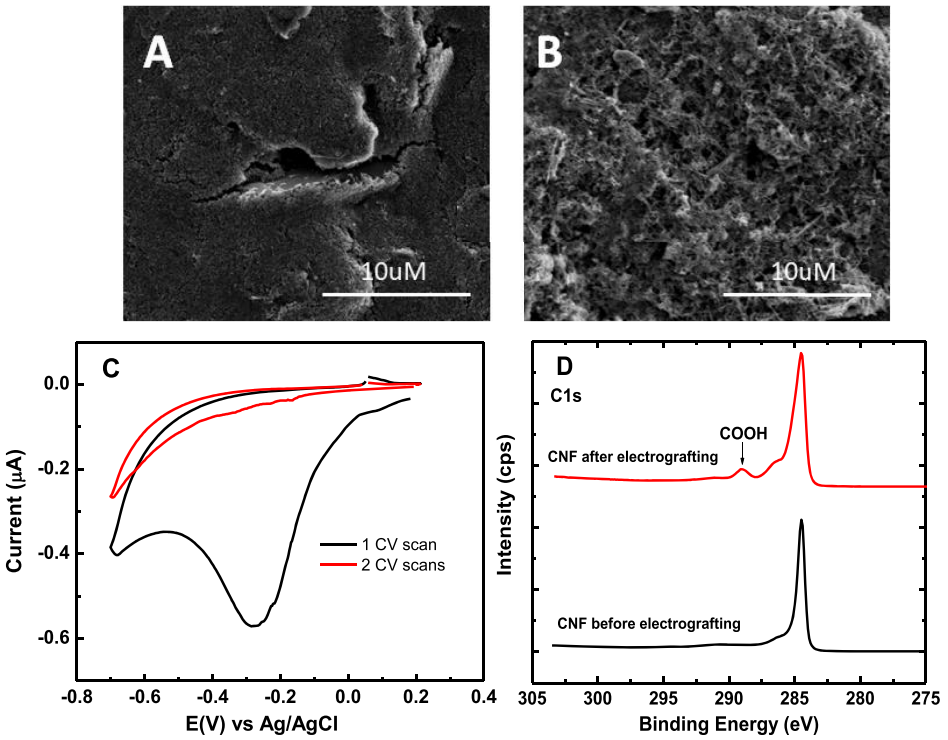

Figure 1. SEM images of the screen-printed carbon electrodes (A) and the carbon electrode after modification with carbon nanofibers (B). The two consecutive cyclic voltammograms of the electrografting step on the CNF electrode (C) (scans were recorded in the diazonium salt solution in HCl at a scan rate of 50 mV s^{-1}). (D) The XPS C 1s high-resolution spectra of the CNF electrodes before and after the electrografting of carboxyphenyl groups.

and mixed with the antibody, then incubated on the sensor surface, as previously explained.

RESULTS AND DISCUSSION

Characterization of the CNF-Modified Electrodes before and after the Electrografting of Carboxyphenyl Moieties. In this work, we used screen-printed carbon electrodes for the sensor fabrication. Commercially available CNF powder in DMF was used to modify the carbon working electrodes. SEM was used to characterize the morphology of the carbon working electrodes and the CNF-modified electrodes. As shown in Figure 1A,B, the SEM images of the carbon and CNF-modified electrodes exhibited different morphologies. The carbon electrode showed a typical multilayered graphitic structure, whereas the CNF electrodes exhibited a densely packed layer of CNF rods, indicating higher surface area of the CNF electrodes compared with the unmodified carbon electrode.

The CNF electrodes were then functionalized by electrografting of carboxyphenyl moieties on the electrode surface. This method has been previously optimized and used for different applications showing excellent stability and simplicity.[28−30] The electrografting was achieved via electroreduction of carboxyphenyl diazonium salt by CV. As shown in Figure 1C, the first CV scan showed a single irreversible cathodic peak at 0.3 V, characteristic for the reduction of diazonium salt via one electron transfer process. The reduction led to the removal of nitrogen molecule and the formation of aryl radical that forms a covalent bond with the CNF surface. However, in the second CV scan, the reduction peak was almost disappeared, likely because of the complete coverage of the CNF electrode surface with the carboxyphenyl layer which retarded the electron transfer process. Further CV scans will lead to a build-up of multilayers which will negatively impact the biosensor performance, as previously reported.[26,27,31] Thus, only two CV scans were performed for the electrografting step to ensure monolayer formation of the carboxyphenyl moieties.

XPS was then used to analyze the CNF electrode surface before and after the electrografting step using CV. Figure 1D shows the XPS C 1s high-resolution spectra of the electrode before and after functionalization. A new peak was observed clearly at 288.8 eV after the electrografting step compared with the spectra of the unmodified CNF electrode which confirms the successful attachment of the carboxyl groups on the CNF surface.

SWV Characterization of the Stepwise Fabrication Process of the Biosensor. To characterize the fabrication steps of the immunosensor, SWVs were recorded at different steps in ferro/ferricyanide solution. Figure 2 shows the SWV reduction peaks of the redox couple at the bare carbon electrode, the CNF-modified electrode, the carboxyphenyl-modified electrode, and after the immobilization of the N protein. As shown in the figure, an enhancement of the reduction peak current was observed when the electrode was modified with CNF compared to the bare carbon electrode. This is attributed to the increase in the electrochemical surface area of the electrode because of the CNF material. However, after the electroreduction step of the diazonium salt on the CNF electrode, the SWV reduction signal of the redox couple was almost disappeared because of the formation of the carboxyphenyl layer on the electrode surface. This has led to the passivation of the electrode and retardation of the electron transfer because of the aromatic layer. Moreover, the negatively charged carboxyl groups repelled the redox anion from the

https://dx.doi.org/10.1021/acs.analchem.0c04719
Anal. Chem. XXXX, XXX, XXX−XXX

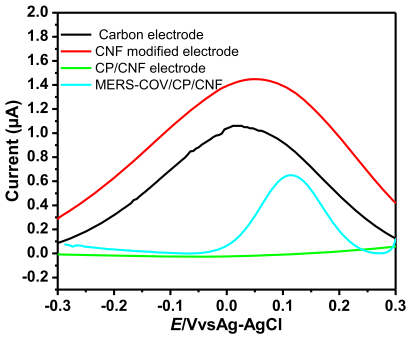

Figure 2. Square wave voltammograms of the bare carbon electrode (black curve), the CNF-modified electrode (red), the carboxyphenyl-modified CNF electrodes (green), and after the immobilization of the SARS-CoV-2 nucleocapsid antigen. The measurements were recorded in 10 mM ferro/ferricyanide redox solution.

surface, leading to a decrease in the reduction current. However, the immobilization of the virus protein antigen on the carboxyphenyl-modified electrode after activation with EDC/NHS led to an increase in the reduction peak current. This is likely because of the shielding of the negatively charged carboxylic groups on the CNF surface with the antigen. It is worth noting that the reported isoelectric point of the N protein is 10.07,[32] indicating that the antigen carries a positive charge at pH 7.4.

Effect of the Cotton Coating on the Electrochemical Signal of the Electrode. The goal of this work is to develop a cotton-tipped electrochemical immunosensor which can perform both the sample collection and the detection. After the immobilization of the protein antigen on the CNF electrode, the electrodes were blocked with BSA solution and left to dry at room temperature. Then, a piece of cotton fiber was coated on the detection zone of the electrode, as shown in Figure 3A, which mimics the standard Q-tip. The cotton was used because of its high absorbing capability which allows the collection of the nasal samples by swabbing.[33] The incubation of the sensor with the antibody solution and the measuring redox solution is carried out in PCR tubes, as shown in Figure 3B,C.

To this end, it was crucial to first investigate whether the coating of the electrode with the cotton fiber impacts the electrochemical signal. Figure 3D shows the SWV reduction peak current of the bare electrode before and after coating with the cotton in the redox solution. Nonsignificant change (less than 5%) in the electrochemical signal was observed after coating the carbon electrode with the cotton, likely because of the high absorbing properties of the cotton fiber. The cotton fiber was able to absorb the redox solution by capillary action and transports it to the electrode surface which remains in contact with the solution during the measurements. Figure 3E shows the reduction peak current at the SARS-CoV-2 immunosensor (the antigen-modified electrode after blocking with BSA) before and after coating with the cotton. The change in the peak current was less than 5%, indicating that there was no significant effect on the electrochemical signal of the sensor because of the coating with the cotton. It was also important to assess the effect of cotton coating on the biosensor response to the binding of the antigen on the sensor surface with the antibody in the solution. For this purpose, the reduction current of the uncoated and cotton-coated immunosensors was detected in the redox solution. Then, the two immunosensors were incubated in 1 ng/mL solution of antibody in two PCR tubes. After washing, the electrodes were measured in the redox solution and the sensor response was evaluated as the percentage change in the reduction peak current in each case. As shown in Figure 3F, the cotton-tipped biosensor response was almost similar to the uncoated immunosensor. These results imply that the cotton-tipped electrochemical sensor can be used as an effective platform with dual function as a sample collector and detection tool.

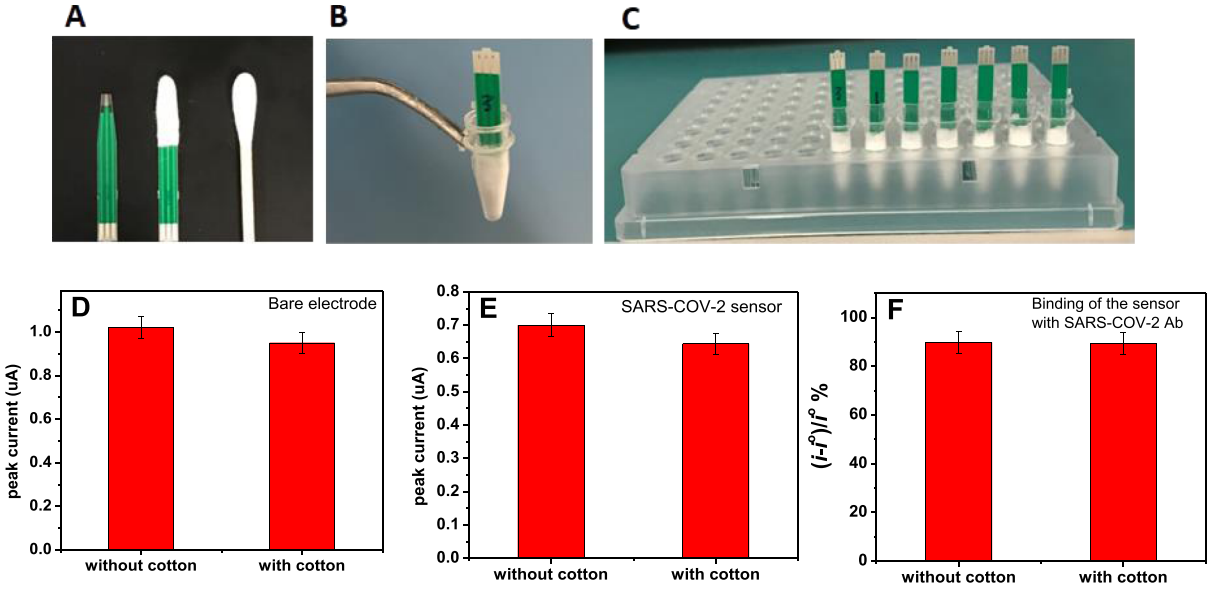

Figure 3. (A) Image of the screen-printed electrode before and after coating with the cotton and scale comparison with a standard Q-tip cotton swab. (B,C) Images of the cotton-tipped electrodes immersed in standard PCR tubes. (D) SWV reduction peak current of the electrode before and after coating with the cotton. (E) SWV reduction peak current of the immunosensor (antigen-modified electrode) before and after coating with the cotton. (F) Immunosensor response toward binding to N antibody with and without coating with the cotton. All the SWV measurements were carried out in 10 mM ferro/ferricyanide solution.

https://dx.doi.org/10.1021/acs.analchem.0c04719
Anal. Chem. XXXX, XXX, XXX−XXX

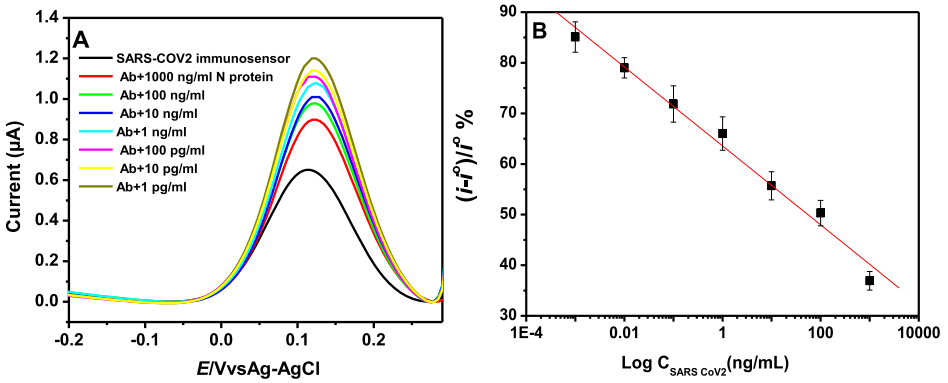

Figure 4. Square wave voltammograms of the SARS-CoV-2 (A) immunosensors before and after binding with different concentrations of nucleocapsid protein mixed with 10 μg/mL nucleocapsid antibody solution. The calibration plot of SARS-CoV-2 (B) detection [plot of the logarithm of the antigen concentration vs the percentage change in the SWV peak current before and after binding $(i - i^{o})/i^{o}$ %]. The error bars show the standard deviations of three measurements.

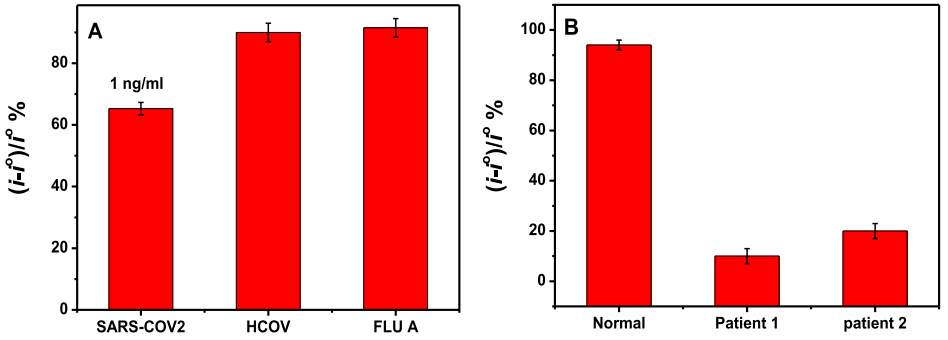

Figure 5. (A) SARS-CoV-2 biosensor response toward the binding with nucleocapsid SARS CoV-2, Flu A, and HCoV antigens. (B) Comparison between the biosensor response signals toward normal and patient samples.

Competitive Electrochemical Detection of SARS-CoV-2 on the Immunosensor. The detection on the immunosensor was achieved via a competitive assay where a fixed concentration of antibody is mixed in the solution with different concentrations (0.1 pg/mL to 1 μg/mL) of the N protein antigen solution and then incubated on the immunosensor surface. A competition between the immobilized and the free antigen to bind the free antibody in the solution is realized. The higher the concentration of free antigen, the smaller the amount of antibody available to bind to the antigen on the electrode surface. The binding of the antibody to the antigen on the immunosensor causes an increase in the reduction peak current of the ferro/ferricyanide redox couple. This could be attributed to the binding with the positively charged antibodies which attract the redox anions, leading to an enhancement of the reduction current.

Figure 4A shows the SWVs of the SARS-CoV-2 immunosensor upon incubation with different concentrations of N protein mixed with 10 μg/mL of the antibody solution. When the concentration of the N protein was high, the increase in the SWV peak current was low and vice versa. The calibration plot of the SARS-CoV-2 immunosensor is shown in Figure 4B. The calibration plot is obtained by plotting the biosensor response [the percentage increase in the peak current; $(i - i^{o})/i^{o}$ %] versus the logarithm of the antigen concentration. Good linear relationship was obtained for the concentration ranges from 1 to 1000 ng/mL of the N protein solution. The linear regression equations of the straight line was $(i - i^{o})/i^{o}$ % = 63.6 + −7.8 log C (ng/mL) (R = 0.991) for SARS-CoV-2. The limit of detection (LOD) was calculated to be 0.8 pg/mL for SARS-CoV-2 N antigen, indicating excellent sensitivity of the immunosensor. This LOD is much lower than that in other reported immunoassays such as enzyme-linked immunosorbent assay (ELISA) (LOD of ELISA is 0.4 ng/mL for SARS-CoV-2 N protein). All the experiments were carried out in triplicates, and the standard deviations of the measurements were ranging from 2.5 to 5.5%, indicating excellent reproducibility of the electrochemical immunosensor.

Cross-Reactivity of the SARS-CoV-2 Immunosensor with Other Virus Antigens. In order to confirm the selectivity of our immunosensor to the SARS-CoV-2 N antigen, the immunosensor was tested against other virus antigens such as Flu A and HCoV. Figure 5A shows the SARS-CoV-2 immunosensor responses against the N antigen as well as HCoV and Flu A. As shown in the figure, significant difference is found between the response of the immunosensor toward its specific and nonspecific antigens. Higher sensor response was obtained in the case of the nonspecific antigens because there were no binding in the solution and thus, the maximum amount of antibody was free to bind to the electrode, whereas lower response was obtained when the specific antigen was used. These results indicate high selectivity of the cotton-tipped SARS-CoV-2 electrochemical immunosensors.

Application of the Cotton-Tipped Immunosensor in Spiked Nasal Samples. To investigate the practical applicability of the developed cotton-tipped electrochemical immunosensor for the detection of the virus in the nasal fluid, the sensor was used to collect the nasal fluid from healthy volunteer and then subjected to the electrochemical measure-

https://dx.doi.org/10.1021/acs.analchem.0c04719
Anal. Chem. XXXX, XXX, XXX−XXX

ments, as described in the Experimental Section. Table 1 shows very good recovery percentages (91−95.5%) of the antigen

Table 1. Real Sample Application of the Immunosensor in Spiked Nasal Samples (n = 3) Showing the Recovery Percentages

spiked antigen (ng/mL)	recovery %	RSD %
0.001	95.5	5.2
100	91	6.0

protein on the cotton immunosensor. This indicates the success of the cotton immunosensor to collect and detect the virus protein with high accuracy and without significant interference from the other component of the nasal fluid.

Application of the Biosensor in Clinical Samples. To investigate the performance of our electrochemical biosensor for the detection of SARS-CoV-2 in clinical samples, nasal swabs from healthy and two patients were collected and stored in UTM. The positive and negative samples were confirmed by performing RT-PCR. The samples were mixed with the antibody and then incubated on the sensor surface for 20 min. The biosensor response was then evaluated for the samples. As shown in Figure 5B, the biosensor response to the patient samples was much lower than the normal healthy sample. These results indicate that our COVID-19 electrochemical biosensor is capable to discriminate between patient and normal samples and showed good agreement with the PCR results.

CONCLUSIONS

To summarize, we developed herein, a cotton-tipped electrochemical immunosensor for the detection of SARS-CoV-2 nucleocapsid virus antigen. Unlike the reported approaches, we integrated the sample collection and detection tools into a single platform by coating screen-printed electrodes with absorbing cotton padding. The immunosensor was fabricated by immobilizing the virus antigen on CNF-modified screen-printed electrodes which were functionalized by diazonium electrografting and activated by EDC/NHS chemistry. The detection of the virus antigen was achieved via swabbing followed by competitive assay using a fixed amount of N protein antibody in the solution. A ferro/ferricyanide redox probe was used for the detection using the SWV technique. The LOD for the N antigen electrochemical immunosensor was 0.8 pg/mL, indicating very good sensitivity for the biosensor. The biosensor did not show cross-reactivity with antigens from other viruses such as influenza A and HCoV, implying high selectivity of the method. Moreover, the biosensor was successfully applied for the detection of the virus antigen in spiked nasal samples showing excellent recovery percentages. The signal measurements can be realized using a handheld potentiostat and easily monitored using a smartphone device. Therefore, the developed cotton based-electrochemical immunosensor is a promising diagnostic tool for the direct, low cost, and rapid detection of the COVID-19 virus which requires no sample transfer or pretreatment. We believe that the identification of other more stable and high-affinity synthetic recognition receptors such as aptamers for the virus proteins will pave the way to replace the antibody in several electrochemical biosensing platforms.

AUTHOR INFORMATION

Corresponding Author

Mohammed Zourob − *Department of Chemistry, Alfaisal University, Riyadh 11533, Saudi Arabia; King Faisal Specialist Hospital and Research Centre, Riyadh 12713, Saudi Arabia;* orcid.org/0000-0003-2187-1430; Email: mzouro@alfaisla.edu

Author

Shimaa Eissa − *Department of Chemistry, Alfaisal University, Riyadh 11533, Saudi Arabia;* orcid.org/0000-0002-5558-0060

Complete contact information is available at: https://pubs.acs.org/10.1021/acs.analchem.0c04719

Notes

The authors declare no competing financial interest.

ACKNOWLEDGMENTS

The authors thank King Abdulaziz City for Science and Technology (KACST) for the financial support to this work through a grant number: 5-20-01-023-0009.

REFERENCES

(1) Sheikhzadeh, E.; Eissa, S.; Ismail, A.; Zourob, M. *Talanta* **2020**, *220*, 121392.
(2) Cui, F.; Zhou, H. S. *Biosens. Bioelectron.* **2020**, *165*, 112349.
(3) Eissa, S.; Zourob, M. *Analyst* **2020**, *145*, 4606−4614.
(4) Eissa, S.; Zourob, M. *Microchim. Acta* **2020**, *187*, 486.
(5) Eissa, S.; Noordin, R.; Zourob, M. *Electroanalysis* **2020**, *32*, 1170−1177.
(6) Abdulhalim, I.; Zourob, M.; Lakhtakia, A. *Electromagnetics* **2008**, *28*, 214−242.
(7) Singh, P. Surface Plasmon Resonance: A Boon for Viral Diagnostics. *Reference Module in Life Sciences*; Elsevier, 2017.
(8) Mauriz, E. *Sensors* **2020**, *20*, 4745.
(9) Das, C. M.; Guo, Y.; Kang, L.; Ho, H. p.; Yong, K. T. *Adv. Theory Simul.* **2020**, *3*, 2000074.
(10) de Eguilaz, M. R.; Cumba, L. R.; Forster, R. J. *Electrochem. Commun.* **2020**, *116*, 106762.
(11) Layqah, L. A.; Eissa, S. *Microchim. Acta* **2019**, *186*, 224.
(12) Kaya, S. I.; Karadurmus, L.; Ozcelikay, G.; Bakirhan, N. K.; Ozkan, S. A. Electrochemical virus detections with nanobiosensors. *Nanosensors for Smart Cities*; Elsevier, 2020; pp 303−326.
(13) Han, M.-Y.; Xie, T.-A.; Li, J.-X.; Chen, H.-J.; Yang, X.-H.; Guo, X.-G. *BioMed Res. Int.* **2020**, *2020*, 3969868.
(14) Hwang, S. G.; Ha, K.; Guk, K.; Lee, D. K.; Eom, G.; Song, S.; Kang, T.; Park, H.; Jung, J.; Lim, E.-K. *Sci. Rep.* **2018**, *8*, 12999.
(15) Seo, G.; Lee, G.; Kim, M. J.; Baek, S.-H.; Choi, M.; Ku, K. B.; Lee, C.-S.; Jun, S.; Park, D.; Kim, H. G.; Kim, S.-J.; Lee, J.-O.; Kim, B. T.; Park, E. C.; Kim, S. I. *ACS Nano* **2020**, *14*, 5135−5142.
(16) Qiu, G.; Gai, Z.; Tao, Y.; Schmitt, J.; Kullak-Ublick, G. A.; Wang, J. *ACS Nano* **2020**, *14*, 5268−5277.
(17) Lin, Q.; Wen, D.; Wu, J.; Liu, L.; Wu, W.; Fang, X.; Kong, J. *Anal. Chem.* **2020**, *92*, 9454−9458.
(18) Grant, B. D.; Anderson, C. E.; Williford, J. R.; Alonzo, L. F.; Glukhova, V. A.; Boyle, D. S.; Weigl, B. H.; Nichols, K. P. *Anal. Chem.* **2020**, *92*, 11305−11309.
(19) Yu, S.; Nimse, S. B.; Kim, J.; Song, K.-S.; Kim, T. *Anal. Chem.* **2020**, *92*, 14139−14144.
(20) Alafeef, M.; Dighe, K.; Moitra, P.; Pan, D. *ACS Nano* **2020**, *14* (12), 17028−17045.
(21) Banks, C. E.; Compton, R. G. *Analyst* **2005**, *130*, 1232−1239.
(22) Huang, J.; Liu, Y.; You, T. *Anal. Methods* **2010**, *2*, 202−211.
(23) Alamer, S.; Eissa, S.; Chinnappan, R.; Herron, P.; Zourob, M. *Talanta* **2018**, *185*, 275−280.

https://dx.doi.org/10.1021/acs.analchem.0c04719
Anal. Chem. XXXX, XXX, XXX−XXX

(24) Alamer, S.; Eissa, S.; Chinnappan, R.; Zourob, M. *Microchim. Acta* **2018**, *185*, 164.
(25) Raji, M. A.; Aloraij, Y.; Alhamlan, F.; Suaifan, G.; Weber, K.; Cialla-May, D.; Popp, J.; Zourob, M. *Talanta* **2021**, *221*, 121468.
(26) Eissa, S.; Jimenez, G. C.; Mahvash, F.; Guermoune, A.; Tlili, C.; Szkopek, T.; Zourob, M.; Siaj, M. *Nano Res.* **2015**, *8*, 1698−1709.
(27) Eissa, S.; Tlili, C.; L'Hocine, L.; Zourob, M. *Biosens. Bioelectron.* **2012**, *38*, 308−313.
(28) Randriamahazaka, H.; Ghilane, J. *Electroanalysis* **2016**, *28*, 13−26.
(29) Bélanger, D.; Pinson, J. *Chem. Soc. Rev.* **2011**, *40*, 3995−4048.
(30) Eissa, S.; Alshehri, N.; Rahman, A. M. A.; Dasouki, M.; Abu-Salah, K. M.; Zourob, M. *Biosens. Bioelectron.* **2018**, *101*, 282−289.
(31) Eissa, S.; L'Hocine, L.; Siaj, M.; Zourob, M. *Analyst* **2013**, *138*, 4378−4384.
(32) Scheller, C.; Krebs, F.; Minkner, R.; Astner, I.; Gil-Moles, M.; Wätzig, H. *Electrophoresis* **2020**, *41*, 1137−1151.
(33) Zasada, A. A.; Zacharczuk, K.; Woźnica, K.; Główka, M.; Ziółkowski, R.; Malinowska, E. *AMB Express* **2020**, *10*, 46.

https://dx.doi.org/10.1021/acs.analchem.0c04719
Anal. Chem. XXXX, XXX, XXX−XXX